# Horizon volumes with interpreted constraints

*Xinming Wu* & Dave Hale*
*Center for Wave Phenomena, Colorado School of Mines, Golden, CO 80401, USA*

## SUMMARY

We propose a method to generate at once an entire volume of horizons in a 3D seismic image. The most significant new aspect of this method is the ability to specify, perhaps interactively during interpretation, a small number of control points that may be scattered throughout a 3D seismic image. Examples show that control points enable the accurate generation of horizon volumes from seismic images in which noise and faults are apparent. These points represent constraints that we implement simply as preconditioners in the conjugate gradient method used to construct horizon volumes.

## INTRODUCTION

Lomask (2010a,b) first presented the concept of a "horizon volume" (Figure 1c), which can be generated from a seismic image (Figure 1a) and used to flatten reflectors (Figure 1d) or to access all horizons at once. A horizon volume $z(x,y,\tau)$ (Figure 1c) contains horizon depth $z$ as a function of relative geologic time (RGT) $\tau$ and spatial coordinates $x$ and $y$. Horizontally slicing a horizon volume yields the spatial locations ($x$, $y$, and $z$) of a horizon corresponding to a constant RGT $\tau$.

The concept of an "RGT volume" (Figure 1b), first presented by Stark (2005), is closely related to the "horizon volume." An RGT volume $\tau(x,y,z)$ (Figure 1b) contains RGT $\tau$ as a function of spatial coordinates $x$, $y$ and $z$. The contours of constant $\tau$ in an RGT volume correspond to seismic horizons. Given an RGT volume $\tau(x,y,z)$ with $\tau$ monotonically increasing with its vertical coordinate $z$, a horizon volume $z(x,y,\tau)$ can be easily obtained by inverse linear interpolation (Parks, 2010).

Methods for obtaining a horizon volume can be generally classified into three categories. The first is stratal slicing (Zeng et al., 1998a,b), which uses several reference horizons to interpolate a set of horizons that form a horizon volume. The second category uses seismic reflector dips (Lomask et al., 2006; Parks, 2010) or *seismic normal vectors* to explicitly (Lomask et al., 2006) or implicitly (Parks, 2010; Luo and Hale, 2012) compute a horizon volume that maps a seismic image from depth domain to a flattened image in RGT domain. The third category (Stark, 2005; Wu and Zhong, 2012a) flattens an entire 3D seismic image using an RGT volume generated by unwrapping a seismic instantaneous phase image.

We propose a method that generates a complete horizon volume constrained by multiple sets of control points. In this method, we first use seismic normal vectors to compute an RGT volume (Figure 1b), from which a horizon volume (Figure 1c) is then interpolated. This process is similar to Parks's (2010) method for flattening a seismic image, but we instead derive the method in a simpler way. Furthermore, we use multiple sets of control points to generate a more accurate horizon volume from a seismic image complicated by faults or noise. Each set of control points belongs to a single horizon with an unspecified RGT value, and is easily specified in seismic interpretation by simply selecting points that we want to lie on the same horizon. We implement these constraints with simple preconditioners in the conjugate gradient (CG) algorithm we use to compute the RGT and horizon volumes.

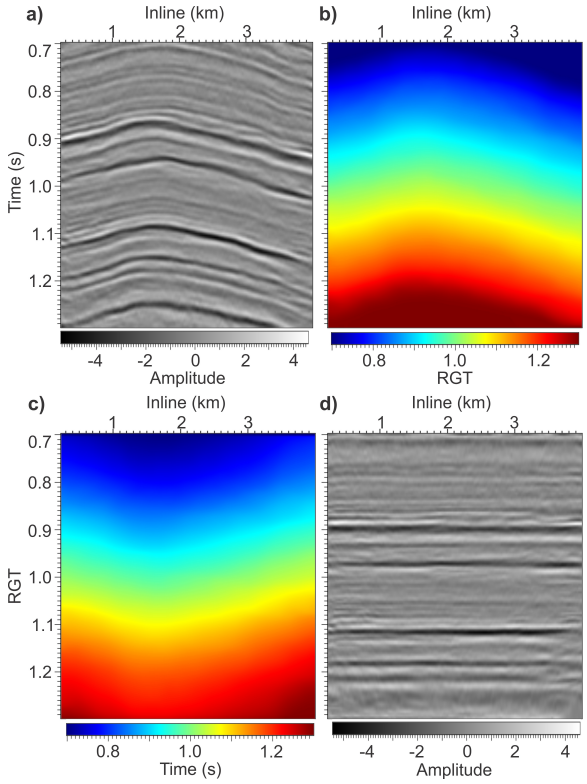


Figure 1: From a seismic image (a), an RGT volume (b) is computed and then converted to a horizon volume (c) that maps the seismic image to a flattened image (d).

## HORIZON VOLUME WITHOUT CONSTRAINTS

A horizon volume $z(x,y,\tau)$ can be generated from an RGT volume $\tau(x,y,z)$ by inverse linear interpolation (Parks, 2010), if we assume that $\tau$ in the RGT volume increases monotonically with depth $z$. Such an RGT volume can be generated by using phase unwrapping (e.g., Stark, 2005; Wu and Zhong, 2012b) or reflector dips (Parks, 2010). Here we rederive the latter method in a simpler way to compute an RGT volume.

In an RGT volume $\tau(x,y,z)$ like that shown in Figure 1b, contours of constant $\tau$ represent seismic horizons, which means these contours should have the same structure as reflectors in

the seismic image (Figure 1a). Therefore, gradient vectors of an RGT volume $\tau(x,y,z)$ that are perpendicular to RGT contours, should be parallel to seismic normal vectors $\mathbf{n} = [n_x, n_y, n_z]^\top$, that are perpendicular to seismic reflectors. If we assume that these vectors always point downward, we then have

$$\begin{bmatrix} \partial\tau/\partial x \\ \partial\tau/\partial y \\ \partial\tau/\partial z \end{bmatrix} \approx \alpha \begin{bmatrix} n_x \\ n_y \\ n_z \end{bmatrix}, \tag{1}$$

where $\alpha$ is a positive scalar constant. To eliminate $\alpha$, we let $\partial\tau/\partial z = \alpha n_z$ to obtain

$$\begin{bmatrix} n_z(\partial\tau/\partial x) - n_x(\partial\tau/\partial z) \\ n_z(\partial\tau/\partial y) - n_y(\partial\tau/\partial z) \end{bmatrix} \approx \begin{bmatrix} 0 \\ 0 \end{bmatrix}. \tag{2}$$

In attempting to solve these equations, we would need to carefully choose boundary conditions to avoid obtaining the trivial solution $\tau = constant$. To avoid this problem, we rewrite $\tau(x,y,z)$ with vertical shifts $s(x,y,z)$ as in Parks (2010):

$$\tau(x,y,z) = z + s(x,y,z). \tag{3}$$

Substituting equation 3 into equation 2, we obtain

$$\begin{bmatrix} -\partial s/\partial x - p(\partial s/\partial z) \\ -\partial s/\partial y - q(\partial s/\partial z) \end{bmatrix} \approx \begin{bmatrix} p \\ q \end{bmatrix}, \tag{4}$$

where $p = -n_x/n_z$ and $q = -n_y/n_z$ are estimated inline and crossline slopes of seismic reflectors. Equation 4 is what Parks (2010) solved to obtain shifts that flatten a seismic image, but we derive it in a simpler way.

As suggested by Lomask et al. (2006), we add a third equation $\varepsilon s_z \approx 0$ ($\varepsilon$ is a small constant) to reduce vertical variations in the shifts. We also weight the equations above by a measure $w(x,y,z)$ of the quality of estimated reflector slopes $p(x,y,z)$ and $q(x,y,z)$. We then compute the shifts by solving

$$\begin{bmatrix} w[-\partial s/\partial x - p(\partial s/\partial z)] \\ w[-\partial s/\partial y - p(\partial s/\partial z)] \\ \varepsilon(\partial s/\partial z) \end{bmatrix} \approx \begin{bmatrix} wp \\ wq \\ 0 \end{bmatrix}. \tag{5}$$

For an image with $N$ samples, equation 5 represents $3N$ equations for $N$ unknown shifts, and these equations can be expressed in matrix form as

$$\mathbf{WGs} = \mathbf{Wv}, \tag{6}$$

where $\mathbf{s}$ is a vector containing $N$ unknown shifts $s(x,y,z)$, $\mathbf{G}$ is a $3N \times N$ matrix representing finite-difference approximations of partial derivatives, $\mathbf{W}$ is a $3N \times 3N$ diagonal matrix containing $w(x,y,z)$ and $\varepsilon$, and $\mathbf{v}$ is a $3N \times 1$ vector with $p$, $q$, and zeros. We compute the least-squares solution to equation 6 by solving the normal equations $(\mathbf{WG})^\top\mathbf{WGs} = (\mathbf{WG})^\top\mathbf{Wv}$. Let $\mathbf{A} = (\mathbf{WG})^\top\mathbf{WG}$ and $\mathbf{b} = (\mathbf{WG})^\top\mathbf{Wv}$, then we solve

$$\mathbf{As} = \mathbf{b}. \tag{7}$$

Because the matrix $\mathbf{A}$ is SPD, we can solve this linear system using the CG method with a preconditioner

$$\mathbf{M^{-1}} = \mathbf{S}_x\mathbf{S}_y\mathbf{S}_z\mathbf{S}_z^\top\mathbf{S}_y^\top\mathbf{S}_x^\top, \tag{8}$$

where $\mathbf{S}_x$, $\mathbf{S}_y$ and $\mathbf{S}_z$ are smoothing filters that smooth in the $x$, $y$ and $z$ directions, respectively. For an image with faults or unconformities, $\mathbf{S}_x$, $\mathbf{S}_y$ and $\mathbf{S}_z$ are designed to be spatially variant filters (Hale, 2009), and the extent of smoothing is controlled by fault (Hale, 2013) or unconformity attributes.

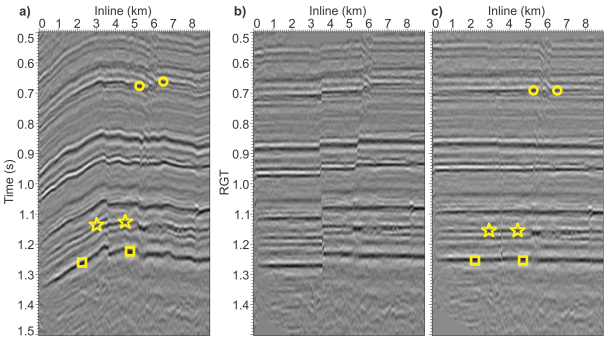


Figure 2: A seismic image (a) is flattened (b) without and (c) with 3 pairs of interactively interpreted control points (yellow circles, stars and squares).

For the 2D example shown in Figure 1, we first solved equation 7 to get shifts $s(x,z)$. We then computed an RGT volume $\tau(x,z) = z + s(x,z)$ (Figure 1b). Finally we computed a horizon volume $z(x,\tau)$ (Figure 1c) from the RGT volume $\tau(x,z)$ by inverse linear interpolation. This horizon volume maps the seismic image (Figure 1a) to a flattened image (Figure 1d). For seismic images with simple geologic structures and little noise, as in Figure 1a, we can use the method discussed above to generate an accurate horizon volume (Figure 1c) that correctly flattens (Figure 1d) a seismic image. However, for a seismic image complicated by faults, as in Figure 2a, the method cannot correctly flatten (Figure 2b) the seismic image. Therefore, we extend this method by incorporating scattered sets of control points that may correspond to multiple horizons.

## HORIZON VOLUME WITH CONSTRAINTS

Solving the linear system in equation 7 is equivalent to minimizing the quadratic function $F(\mathbf{s}) = \frac{1}{2}\mathbf{s}^\top\mathbf{As} - \mathbf{b}^\top\mathbf{s}$ because $\mathbf{A}$ is SPD. With specified sets of control points, we solve a constrained minimization problem

$$\begin{aligned} &\text{minimize}_{\mathbf{s}} \quad F(\mathbf{s}) = \frac{1}{2}\mathbf{s}^\top\mathbf{As} - \mathbf{b}^\top\mathbf{s}, \\ &\text{subject to} \quad \mathbf{Cs} = \mathbf{d}, \end{aligned} \tag{9}$$

where matrix $\mathbf{C}$ and vector $\mathbf{d}$ are derived from constraints. As discussed by Gould et al. (2001), solving this constrained minimization problem is equivalent to solving the unconstrained linear system $\mathbf{As} = \mathbf{b}$ using a CG method with an initial solution $\mathbf{s}_0$ satisfying the constraint equation $\mathbf{Cs}_0 = \mathbf{d}$ and a constraint preconditioner $\mathbf{P} = \mathbf{Z}(\mathbf{Z}^\top\mathbf{AZ})^{-1}\mathbf{Z}^\top$, where $\mathbf{Z}$ is a matrix whose columns form a basis for the null space of $\mathbf{C}$ ($\mathbf{CZ} = \mathbf{0}$). Since columns of $\mathbf{Z}$ form a basis, then we have $\mathbf{Z}^\top\mathbf{Z} = \mathbf{I}$ and we use $\mathbf{Z}^\top\mathbf{M}^{-1}\mathbf{Z} \approx (\mathbf{Z}^\top\mathbf{AZ})^{-1}$ as in Nash and Sofer (1996) to simplify the preconditioner $\mathbf{P}$:

$$\mathbf{P} = \mathbf{ZZ}^\top\mathbf{M}^{-1}\mathbf{ZZ}^\top, \tag{10}$$

where $\mathbf{M}^{-1}$ is an approximate inverse of matrix $\mathbf{A}$ and we use $\mathbf{M^{-1}} = \mathbf{S}_x\mathbf{S}_y\mathbf{S}_z\mathbf{S}_z^\top\mathbf{S}_y^\top\mathbf{S}_x^\top$ as in equation 8. Therefore, to solve

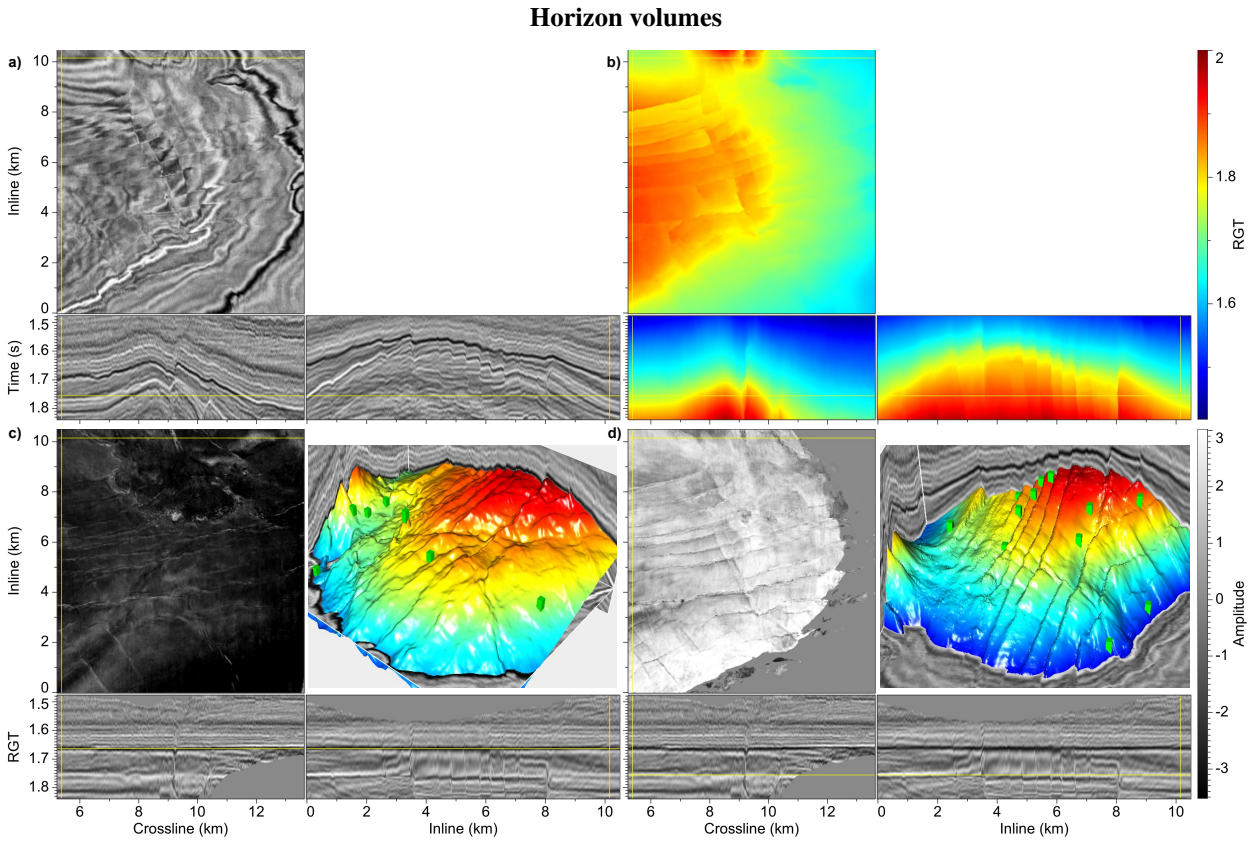


Figure 3: A 3D seismic image image (a), the corresponding RGT volume (b) computed with 3 sets of control points, and the flattened image sliced at $\tau = 1.666$ (c) and $\tau = 1.758$ (d). Horizontal slices in flattened images correspond to horizon surfaces (upper-right panels in (c) and (d), for which color denotes depth) in unflattened images.

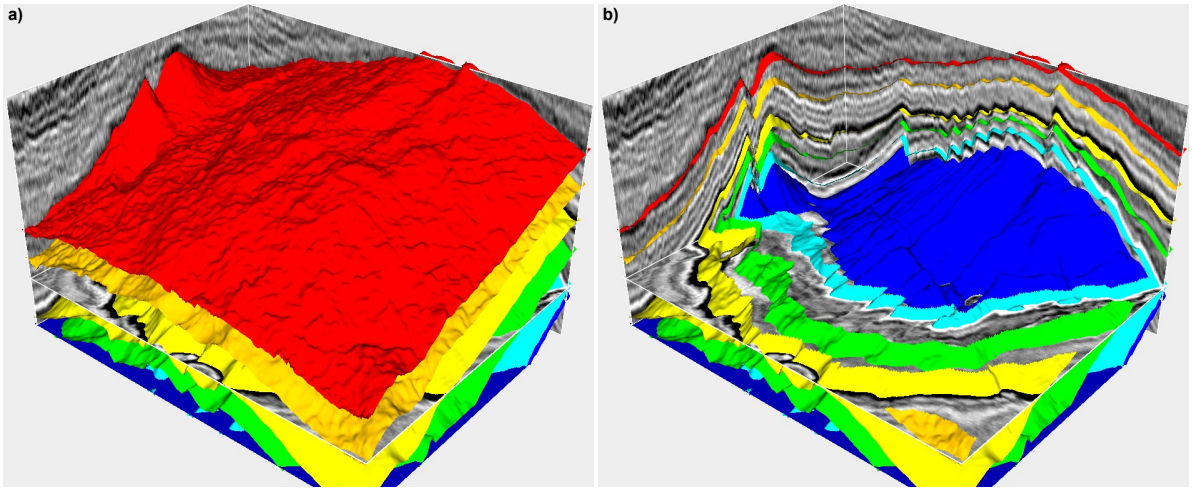


Figure 4: A 3D view of 6 seismic horizons (a) with different colors, and cut-away views (b) of the horizons to show more details. These horizons are a small subset of those in a complete horizon volume.

this problem, we need only an initial solution $\mathbf{s}_0$ satisfying the constraint equation $\mathbf{C}\mathbf{s}_0 = \mathbf{d}$ and the matrix $\mathbf{Z}\mathbf{Z}^\top$ for the constraint preconditioner $\mathbf{P}$.

Let us use a tiny 3D seismic image with only $N = 2 \times 2 \times 2$ samples to explain how to implement multiplication by the matrix $\mathbf{Z}\mathbf{Z}^\top$ and to find an initial solution $\mathbf{s}_0$. In this example, the RGT volume $\tau(x,y,z)$ and shifts $s(x,y,z)$ have only $N = 8$ samples, and equation 3 can be expressed in vector form as

$$\begin{aligned}[\tau_0\ \tau_1\ \tau_2\ \tau_3\ \tau_4\ \tau_5\ \tau_6\ \tau_7]^\top &= [z_0\ z_1\ z_2\ z_3\ z_4\ z_5\ z_6\ z_7]^\top \\ &+ [s_0\ s_1\ s_2\ s_3\ s_4\ s_5\ s_6\ s_7]^\top .\end{aligned} \tag{11}$$

Assume we have 2 sets of constraints: the first set has 3 control points with sample indices $\{3,5,7\}$, and the second has 2 control points with sample indices $\{1,6\}$. Within each set of constraints, all control points are interpreted to be on a single seismic horizon. Therefore, we have $\tau_3 = \tau_5 = \tau_7$ and $\tau_1 = \tau_6$. According to equation 11, this means that $s_5 - s_3 = z_3 - z_5$, $s_7 - s_3 = z_3 - z_7$, and $s_6 - s_1 = z_1 - z_6$. We can therefore write the constraint equation $\mathbf{Cs} = \mathbf{d}$ as follows:

$$\begin{bmatrix} 0 & 0 & 0 & -1 & 0 & 1 & 0 & 0 \\ 0 & 0 & 0 & -1 & 0 & 0 & 0 & 1 \\ 0 & -1 & 0 & 0 & 0 & 0 & 1 & 0 \end{bmatrix} \mathbf{s} = \begin{bmatrix} z_3 - z_5 \\ z_3 - z_7 \\ z_1 - z_6 \end{bmatrix}. \quad (12)$$

Given matrix $\mathbf{C}$ as shown in the left hand side of equation 12, a corresponding matrix $\mathbf{Z}$, whose columns form a basis for the null space of $\mathbf{C}$ such that $\mathbf{CZ} = \mathbf{0}$, can be constructed by

$$\mathbf{Z} = \left[\mathbf{e}_{c1} \mid \mathbf{e}_{c2} \mid \mathbf{e}_0 \mid \mathbf{e}_2 \mid \mathbf{e}_4\right] = \begin{bmatrix} 0 & 0 & 1 & 0 & 0 \\ 0 & 1 & 0 & 0 & 0 \\ 0 & 0 & 0 & 1 & 0 \\ 1 & 0 & 0 & 0 & 0 \\ 0 & 0 & 0 & 0 & 1 \\ 1 & 0 & 0 & 0 & 0 \\ 0 & 1 & 0 & 0 & 0 \\ 1 & 0 & 0 & 0 & 0 \end{bmatrix}_{8\times 5}, \quad (13)$$

where $\mathbf{e}_i$ ($i = 0, 1, \cdots, N-1$) is an $N \times 1$ unit vector with 1 at the $i-th$ index, $\mathbf{e}_{c1} = \mathbf{e}_3 + \mathbf{e}_5 + \mathbf{e}_7$, and $\mathbf{e}_{c2} = \mathbf{e}_1 + \mathbf{e}_6$. In other words, we begin with the identity matrix and simply sum the unit vectors $\mathbf{e}_i$ with indices $i$ in $\{3,5,7\}$, corresponding to the first set of control points, to obtain the first column of $\mathbf{Z}$; similarly, we obtain the second column of $\mathbf{Z}$, corresponding to the second set of control points with indices $\{1,6\}$; and finally, we use all of the remaining unit vectors $\mathbf{e}_i$ that do not correspond to any control point for remaining columns of $\mathbf{Z}$. In the same way, we can easily construct matrix $\mathbf{Z}$ for any number of sets of control points. We further normalize each column of matrix $\mathbf{Z}$ and such that $\mathbf{Z}^\top\mathbf{Z} = \mathbf{I}$ and $\mathbf{ZZ}^\top$ is

$$\mathbf{ZZ}^\top = \begin{bmatrix} 1 & 0 & 0 & 0 & 0 & 0 & 0 & 0 \\ 0 & \frac{1}{2} & 0 & 0 & 0 & 0 & \frac{1}{2} & 0 \\ 0 & 0 & 1 & 0 & 0 & 0 & 0 & 0 \\ 0 & 0 & 0 & \frac{1}{3} & 0 & \frac{1}{3} & 0 & \frac{1}{3} \\ 0 & 0 & 0 & 0 & 1 & 0 & 0 & 0 \\ 0 & 0 & 0 & \frac{1}{3} & 0 & \frac{1}{3} & 0 & \frac{1}{3} \\ 0 & \frac{1}{2} & 0 & 0 & 0 & 0 & \frac{1}{2} & 0 \\ 0 & 0 & 0 & \frac{1}{3} & 0 & \frac{1}{3} & 0 & \frac{1}{3} \end{bmatrix}_{8\times 8}. \quad (14)$$

For any vector $\mathbf{x} = [x_0\ x_1\ x_2\ x_3\ x_4\ x_5\ x_6\ x_7]^\top$, it is easy to compute the matrix-vector product

$$\mathbf{ZZ}^\top\mathbf{x} = [x_0\ x_{c2}\ x_2\ x_{c1}\ x_4\ x_{c1}\ x_{c2}\ x_{c1}]^\top, \quad (15)$$

where $x_{c1} = (x_3 + x_5 + x_7)/3$ and $x_{c2} = (x_1 + x_6)/2$. In other words, we compute $\mathbf{ZZ}^\top\mathbf{x}$ by simply gathering and averaging all elements of $\mathbf{x}$ with indices corresponding to each set of control points, and then scattering the average back into those same elements. In each CG iterate, when we apply the constraint preconditioner $\mathbf{P} = \mathbf{ZZ}^\top\mathbf{S}_x\mathbf{S}_y\mathbf{S}_z\mathbf{S}_z^\top\mathbf{S}_y^\top\mathbf{S}_x^\top\mathbf{ZZ}^\top$, we need only compute averages and apply smoothing filters.

We can also easily find an initial solution $\mathbf{s_0}$ satisfying the constraint equation $\mathbf{Cs_0} = \mathbf{d}$:

$$\mathbf{s_0} = [0\ s_1\ 0\ s_3\ 0\ s_5\ s_6\ s_7]^\top, \quad (16)$$

in which elements with indices corresponding to the first set of control points are $s_3 = 0$, $s_5 = z_3 - z_5$ and $s_7 = z_3 - z_7$; elements corresponding to the second set are $s_1 = 0$ and $s_6 = z_1 - z_6$. Therefore, to construct $\mathbf{s}_0$, we use zeros for elements that do not correspond to any control point; for each set of control points, we choose any point among them as a reference point with zero shift (e.g., $s_3 = 0$ for the first set, and $s_1 = 0$ for the second set), and use the depth differences between the reference point and other control points for the remaining initial shifts in $\mathbf{s}_0$.

Figure 2 is a 2D example that shows how constraints help to generate a more accurate horizon volume or better flatten a seismic image. In this example, the method without control points cannot correctly flatten the image (Figure 2b), especially at faults. However, using 3 sets of constraints, each set contains 2 control points (yellow circles, stars, and squares in Figures 2a and 2c) that lie on a seismic horizon, our method correctly flattens (Figure 2c) all seismic reflectors across faults.

Figure 3 shows a 3D example with three sets of constraints, corresponding to three horizons in the seismic image. The first set contains 5 control points, the second one contains 7 control points (green points in Figure 3c), and the third one contains 11 control points (green points in Figure 3d). With these constraints, our method correctly flattens all of the seismic reflectors across faults, as shown in Figures 3c or 3d. Note that the constraints help to flatten not only reflectors passing through the control points, but also other reflectors in the 3D seismic image as well. Seismic horizon surfaces (upper-right panels of Figures 3a and 3b) can be extracted by horizontally slicing at the flattened image. Figure 4a displays six extracted horizons denoted by different colors, but deeper horizons are obscured by the top one. We therefore, in Figure 4b, display cut-away views of each of the horizons. We observe that the horizons with control points (the cyan and yellow surfaces) and others without control points correctly align with seismic reflectors.

## CONCLUSION

We propose a method to compute at once a complete horizon volume that honors interpreted sets of control points. We incorporate the constraints with a simple constraint preconditioner in the CG method used to compute a horizon volume.

To extract complicated seismic horizons, interpreted constraints are usually necessary. The proposed method provides an especially simple way to specify such constraints by simply picking control points in a 3D seismic image that belong to the same seismic horizon. This method can be implemented to interactively add or move control points, while quickly updating a complete horizon volume.

## ACKNOWLEDGMENTS

This research is supported by the sponsor companies of the Consortium Project on Seismic Inverse Methods for Complex Structures. Seismic images shown in this paper were provided by the US Department of Energy and by dGB Earth Sciences.

## REFERENCES


Dollar, H., 2005, Iterative linear algebra for constrained optimization: Ph.D. Thesis, University of Oxford.

Farnebäck, G., J. Rydell, T. Ebbers, M. Andersson, and H. Knutsson, 2007, Efficient computation of the inverse gradient on irregular domains: 2007 IEEE 11th International Conference on Computuer Vision, Vols 1-6, IEEE, 2710–2717.

Gould, N. I. M., M. E. Hribar, and J. Nocedal, 2001, On the solution of equality constrained quadratic programming problems arising in optimization: SIAM J. Sci. Comput., **23**, 1376–1395.

Hale, D., 2009, Structure-oriented smoothing and semblance: CWP Report 635.

———, 2013, Methods to compute fault images, extract fault surfaces, and estimate fault throws from 3d seismic images: Geophysics, **78**, O33–O43.

Harlan, W. S., 1995, Regularization by model reparameterization: http://www.billharlan.com/papers/regularization.pdf.

Lomask, J., 2010a, Method for determinint geological information related to a subsurface volume of interest: U. S. Patent 7,769,545 B2.

———, 2010b, Method for indexing a subsurface for the purpose of inferring geologic information: U. S. Patent 7,769,546 B2.

———, 2013, System and method for perturbing an initial horizon-picking solution to follow local features of a volume: U. S. Patent 2013/0030710 A1.

Lomask, J., A. Guitton, S. Fomel, J. Claerbout, and A. A. Valenciano, 2006, Flattening without picking: Geophysics, **71**, 13–20.

Luo, S., and D. Hale, 2012, Unfaulting and unfolding 3D seismic images: CWP Report 722.

Fehmers, G. C., and C. Höcker, 2003, Fast structural interpretation with structure-oriented filtering: Geophysics, **68**, 1286–1293.

Nash, S. G., and A. Sofer, 1996, Preconditioning reduced matrices: SIAM J. Matrix Anal. Appl., **17**, 21–34.

Parks, D., 2010, Seismic image flattening as a linear inverse problem: M.S. Thesis, Colorado School of Mines.

Posamentier, H., R. Davies, J. Cartwright, and L. Wood, 2007, Seismic geomorphology - an overview: in: R.J. Davies, H.W. Posamentier, L.J. Wood, J.A. Cartwright (Eds.), Seismic Geomorphology, Geological Society of London Special Publication, 1–14.

Saad, Y., 1996, Iterative methods for sparse linear systems: PWS Publishing Company, Boston.

Stark, T. J., 2005, Generating a seismic Wheeler volume: 75th Ann. Internat. Mtg., Soc. of Expl. Geophys., 782–785.

Vail, P. R., R. G. Todd, and J. B. Sangree, 1977, Seismic stratigraphy and global changes of sea level: Part 5. chronostratigraphic significance of seismic reflections: Section 2. application of seismic reflection configuration to stratigraphic interpretation: M 26: Seismic Stratigraphy-Applications to Hydrocarbon Exploration, AAPG Memoirs, 99–116.

van Vliet, L. J., and P. W. Verbeek, 1995, Estimators for orientation and anisotropy in digitized images: ASCI95, Proc. First Annual Conference of the Advanced School for Computing and Imaging (Heijen, NL, May 16-18), ASCI, 442–450.

Wu, X., and G. Zhong, 2012a, Generating a relative geologic time volume by 3D graph-cut phase unwrapping method with horizon and unconformity constraints: Geophysics, **77**, 21–34.

———, 2012b, A method for generating a seismic Wheeler volume via a relative geologic time volume: 82nd Ann. Internat. Mtg, Soc. of Expl. Geophys., 1–5.

Zeng, H., M. M. Backus, K. T. Barrow, and N. Tyler, 1998a, Stratal slicing; Part 1, Realistic 3-D seismic model: Geophysics, **63**, 502–513.

Zeng, H., S. C. Henry, and J. P. Riola, 1998b, Strata slicing; Part ii, Real 3-D seismic data: Geophysics, **63**, 514–522.